is a small difference in the bend. Again, the difference between the advancing front theory and the Graetz and Levêque solutions (which is applicable to $Q = 0$) is small. As a consequence, the Graetz-Lévêque solution on this type of plot can also be used for reactive problems ($Q > 0$) with an expected difference with the advancing front theory of 11 to 15% maximum.

NOTATION

C = concentration of oxygen (A) in the fluid, moles/cm^3
C_i = initial value of C, moles/cm^3
C_o = value of C at $x = 0$ and $x = 2d$, moles/cm^3
C_B = cup mixing concentration of oxygen (A), defined by Equation (13), moles /cm^3
c_T = total concentration of B in all forms in the fluid, moles/cm^3
$2d$ = film thickness, cm
D_c = diffusion coefficient of oxygen (A) in the fluid, cm^2/s
D_{Hb} = diffusion coefficient of hemoglobin (B) in the fluid, cm^2/s
k_z = local mass transfer coefficient, defined by Equation (15), cm/s
v_z = velocity of fluid in the z direction, cm/s
v_{av} = average velocity of blood in the z direction,

$$= \frac{1}{d}\int_0^d v_z \cdot dx, \text{ cm/s}$$

x = distance in the transverse direction, cm
z = distance in the direction of flow, cm
z^* = Graetz number
ξ = thickness of the saturated layer, cm

Dimensionless Quantities

C^* = C/C_o
c_T^* = $4c_T/C_o$
D^* = $D_{Hb} \cdot c_T^*/D_c$
E = enhancement factor, defined by Equation (20)
p = dimensionless thickness of saturated layer, $p = \xi/d$
Q = reaction strength parameter, defined by Equation (11)
S = fractional saturation of total B in AB form
S_i = initial value of S
$\overline{S}$ = mixing cup S
Sh_z = local Sherwood Number, defined by Equation (16)
v^* = v_z/v_{av}
y = x/d
z^* = $\dfrac{zD_c}{v_{av}d^2}$

LITERATURE CITED

Buckles, R. G., E. W. Merrill, and E. R. Gilliland, "An Analysis of Oxygen Absorption in a Tubular Membrane Oxygenator," *AIChE J.*, **14**, 703 (1968).

Colton, C. K., K. A. Smith, P. Stroeve, and E. W. Merrill, "Laminar Flow Mass Transfer in a Flat Duct with Permeable Walls," *ibid.*, **17**, 773 (1971).

Danckwerts, P. V., *Gas-Liquid Reactions*, McGraw-Hill, New York (1970).

Dorson, W. J., "Oxygenation of Blood for Clinical Applications," in *Blood Oxygenation*, E. D. Hershey, ed., Plenum Press, New York (1970).

Dorson, W. J. and M. E. Voorhees, "Analysis of Oxygen and Carbon Dioxide Transfer in Membrane Lungs," in *Membrane Lungs and Acute Respiratory Failure*, W. M. Zapol and J. Quist, ed., p. 43, Hemisphere, Washington, D.C. (1976).

Hill, A. V., "Diffusion of Oxygen and Lactic Acid Through Tissues," *Proc. Royal Soc. London, Ser.*, **B104**, 39 (1928).

Lightfoot, E. N., "Low Order Approximations for Membrane Blood Oxygenators," *AIChE J.*, **14**, 669 (1968).

Spaan, J. A. E., "Transfer of Oxygen into Hemoglobin Solution," *Pflügers. Arch.*, **342**, 289 (1973).

Manuscript received November 9, 1978, and accepted March 20, 1979.

Transient and Steady State Characteristics of a Gaseous Reactant in Catalytic Fluidized-Bed Reactors

LIANG-SHIH FAN and L. T. FAN

Department of Chemical Engineering
Kansas State University
Manhattan, Kansas 66506

Many models have been proposed for describing the performance of a fluidized-bed reactor. These include two-phase models (Kato and Wen, 1969; Fryer and Potter, 1972*a*) and three-phase models (Kunii and Levenspiel, 1968; Fryer and Potter, 1972*b*). More often than not, a simplified flow pattern of plug flow or complete mixing is assumed in representing the fluid flow behavior in one or more of the phases in these models. Furthermore, little has been done in understanding the transient aspect of these models.

Gwyn et al. (1970) considered the transient behavior of the upward and downward flow of gas reactants and solid catalyst in the emulsion phase of the fluidized bed. They assumed that the flow pattern in all phases is plug flow type, the chemical reaction is linear, and physical properties are constant along the bed. Fan and Fan

Detailed information regarding numerical values for simulation can be obtained from the authors.

(1978) considered the axial dispersion in the three phases for the nonlinear catalytic reactions in a fluidized bed. The physical properties along the axial coordinate are invariant. Transient characteristics of the gas reactant and the length of the transient period have been examined based on the model.

This note is a sequel to the earlier work by Fan and Fan (1978). The variation of various physical properties along the axial coordinate is considered in the model. The effects of the axial dispersion and rate of chemical reaction on the transient characteristics are analyzed and graphically presented.

MODEL

Suppose that the bubbles, cloud wakes, and emulsion are homogeneously distributed statistically in a fluidized bed, and that each of the three phases, namely, the bubble, cloud wake, and emulsion phases, can be represented by the so-called axial dispersion model. Then we can write equations, in dimensionless form, as

$$\epsilon_{ig}\left(\frac{U_0}{U_{i0}}\right)\left(\frac{\partial \overline{C}_i}{\partial \theta}\right) = \frac{1}{\delta_i Pe_i}\frac{\partial}{\partial \xi}\left[\delta_i \epsilon_{ig}\left(\frac{E_i}{E_{i0}}\right)\frac{\partial \overline{C}_i}{\partial \xi}\right] - \frac{1}{\delta_i}\frac{\partial}{\partial \xi}\left[\delta_i \epsilon_{ig}\overline{C}_i\overline{U}_i\right] - \overline{F}_{i(i+1)}(\overline{C}_i - \overline{C}_{i+1})\left(\frac{\delta_1}{\delta_i}\right) + \overline{F}_{(i-1)i}(\overline{C}_{i-1} - \overline{C}_i)\left(\frac{\delta_1}{\delta_i}\right)\left(\frac{U_{(i-1)0}}{U_{i0}}\right) - \epsilon_{is}\phi\,\overline{C}_i^{\,n}\left(\frac{U_0}{U_{i0}}\right) \quad (1)$$

where

$i = 1$ for the bubble phase

$i = 2$ for the cloud phase

$i = 3$ for the emulsion phase

The initial condition is given as

$$\theta = 0; \quad C_i = \frac{C_{iI}}{C_0} \quad (2)$$

and the boundary conditions are those of the Danckwerts type (Danckwerts, 1953); that is

$$\xi = 0; \quad 1 = \overline{C}_i - \frac{1}{Pe_i}\frac{\partial \overline{C}_i}{\partial \xi}$$

$$\xi = 1; \quad \frac{\partial \overline{C}_i}{\partial \xi} = 0 \quad (3)$$

As presented below, many of the parameters in the model are expressed in SI units in terms of a relatively small number of fundamental parameters that characterize either the bubbling phenomenon or the mass conservation

1. Superficial velocity of the gas in the bubble phase U_{1s} (Toomey and Johnstone, 1952):

$$U_{1s} = U_0 - U_{mf} \quad (4)$$

2. Bubble diameter D_1 (Mori and Wen, 1975):

$$D_1 = D_{1M} - (D_{1M} - D_{10})\exp(-0.3\,x/D_t) \quad (5a)$$

The initial bubble diameter D_{10}, formed at the surface of the perforated plate, is

$$D_{10} = 0.871\,[A_t\,(U_0 - U_{mf})/N_d]^{0.4} \quad (5b)$$

The value of D_{10} for the porous plate distributor can be evaluated from

$$D_{10} = 0.376(U_0 - U_{mf})^2 \quad (5c)$$

The maximum bubble size D_{1M} can be expressed, in SI units, as

$$D_{1M} = 1.64\,[A_t(U_0 - U_{mf})]^{0.4} \quad (5d)$$

When the maximum bubble diameter calculated by Equation (5d) exceeds the bed diameter, the former is substituted by the latter.

3. Rising velocity of bubbles U_1 (Davidson and Harrison, 1963):

$$U_1 = U_0 - U_{mf} + 0.71\,(gD_1)^{0.5} \quad (6)$$

4. Fraction of the bubble phase δ_1:

$$\delta_1 = \frac{U_{1s}}{U_1(1 - \epsilon_{1s})} \quad (7)$$

The fraction of solid particles in the bubble phase has been reported to range from 0.001 to 0.01 (Yoshida et al., 1973).

5. Fraction of the cloud wake phase δ_2 (Murray, 1965; Horio and Wen, 1977):

$$\delta_2 = \left(\frac{U_{mf}}{\epsilon_{mf}\,U_1 - U_{mf}}\right)\delta_1 \quad (8)$$

6. Fraction of the emulsion phase δ_3:

$$\delta_3 = 1 - \delta_1 - \delta_2 \quad (9)$$

7. Superficial velocity of the gas in the cloud phase U_{2s}:

$$U_{2s} = \frac{\delta_2\,\epsilon_{2g}}{\delta_1\,\epsilon_{1g}}\,U_{1s} \quad (10)$$

8. Superficial velocity U_{3s} and linear velocity U_3 of the gas in the emulsion phase:

$$U_{3s} = U_{mf} - U_{2s} \quad (11a)$$

and

$$U_3 = \frac{U_{3s}}{\delta_3\,\epsilon_{3g}} \quad (11b)$$

Note that when the wake volume is small, the effect of solid circulation can be neglected. Thus, the relative velocity of the gas to the solid in the emulsion phase may directly be represented by Equation (11b). From Equations (10), (11a), and (11b), U_3 can be expressed as

$$U_3 = \frac{U_{mf}}{\epsilon_{3g}}\left[\frac{\epsilon_{1g}(\epsilon_{mf}\,U_1 - U_{mf}) - U_{1s}\,\epsilon_{2g}}{\epsilon_{1g}(\epsilon_{mf}\,U_1 - U_{mf}) - U_{1s}\,\epsilon_{mf}}\right] \quad (11c)$$

If ϵ_{2g} is equal to the void fraction at the minimum fluidization state ϵ_{mf}, the following relationship holds:

$$U_3 = \frac{U_{mf}}{\epsilon_{3g}} \quad (11d)$$

9. Height of bed expansion H:

$$H = H_0\left[\frac{1 - \epsilon_I}{1 - \frac{1}{H}\int_0^H (\epsilon_{1g}\delta_1 + \epsilon_{2g}\delta_2 + \epsilon_{3g}\delta_3)\,dx}\right] \quad (12)$$

10. Peclet number. Examination of the available data for the axial dispersion of gases in the emulsion phase

(Muchi et al., 1961; Zuiderweg, 1967) indicates that the axial dispersion coefficient is approximately linearly proportional to the superficial velocity over wide ranges of the operating conditions. If we extend this relationship to the axial dispersion in the bubble phase and to that in the cloud wake phase, the value of Pe_{i0}, defined as U_0H_I/E_{i0}, for the three phases can be considered constant. Pe_i can be related to Pe_{i0} by

$$Pe_i = Pe_{i0}\overline{H} \tag{13}$$

It is further assumed that E_i is equal to E_{i0}.

11. Gas exchange coefficients (Kunii and Levenspiel, 1968):

$$F_{12} = 4.5\left(\frac{U_{mf}}{D_1}\right) + 5.85\left(\frac{g^{0.25}D_G{}^{0.5}}{D_1{}^{1.25}}\right) \tag{14a}$$

$$F_{23} = 6.78\left(\frac{\epsilon_{mf}D_GU_1}{D_1{}^3}\right)^{0.5} \tag{14b}$$

Note that $F_{01} = 0$ and $F_{34} = 0$.

The gas concentration average over the cross-sectional area of the bed $\overline{C}_{avg}$ is

$$\overline{C}_{avg} = \overline{C}_1\delta_1 + \overline{C}_2\delta_2 + \overline{C}_3\delta_3 \tag{15a}$$

The volumetric average gas concentration at the exit of the bed $\overline{C}_H$ can be expressed by

$$\overline{C}_H = \overline{C}_1\frac{U_{1s}}{U_0} + \overline{C}_2\frac{U_{2s}}{U_0} + \overline{C}_3\frac{U_{3s}}{U_0} \tag{15b}$$

The overall conversion of the gas reactant is defined as

$$\overline{X} = 1 - \overline{C}_H \tag{16}$$

METHOD OF SOLUTION

The nonlinear partial differential equations resulting from the volume reaction model were solved using software developed by Sinovec and Madsen (1975). This software package uses second-order finite-difference formulas to discretize the spatial variable. The resulting set of time dependent ordinary differential equations are solved with an integrator of the type developed by Gear (1971). The relative error bound for the time integration process employed in the present calculation was 10^{-4}. The number of spatial meshes specified for this calculation was 51 (or $h = 0.02$). The use of mesh spacing less than 0.02 yielded essentially identical results.

RESULTS AND DISCUSSION

Equation (1) is numerically solved subject to the initial conditions, Equation (2), and the boundary conditions, Equation (3), according to the method presented previously.

As indicated by Equation (12), the height of a fluidized bed is an implicit function of $(\epsilon_{ig}\delta_i)$ which varies along the bed axis. Therefore, to calculate the height of the fluidized bed, a trial and error procedure is required.

Effects of gas mixing in the emulsion phase for a fast reaction. Figure 1*a* shows the transient gas reactant concentration in each phase and the cross-sectional average and volumetric average concentrations at the exit of the reactor for kC_0 as large as 15 s^{-1}. Figure 1*b* shows the steady state profiles of the gas reactant concentration in each phase and the cross-sectional average and volumetric average concentration in the reactor for kC_0 of 15 s^{-1}. It can be seen from Figure 1*a* that the gas reactant concentration in the emulsion phase for a small Pe_{30} is greater than that for a large Pe_{30} at any given time θ. The same results are observed for the gas reactant concentration in the cloud wake phase. The situation is reversed, however, for the gas reactant concentration in the bubble phase and the cross-sectional average and volumetric average concentrations. The volumetric average gas concentration does not vary significantly with respect to Pe_{30}. This is because U_0/U_{mf} for this system is as large as 10, indicating that the flow rate in the emulsion phase is small compared to that in the bubble phase.

The time required to reach the steady state $\theta_{s.s.}$ is defined to satisfy the following two conditions:

$$\frac{C_{avg}\big|_{\xi=0.1,\,\theta=\theta} - C_{avg}\big|_{\xi=0.1,\,\theta=\theta-\Delta\theta}}{\overline{C}_{avg}\big|_{\xi=0.1,\,\theta=\theta}} \leq 0.002 \tag{17}$$

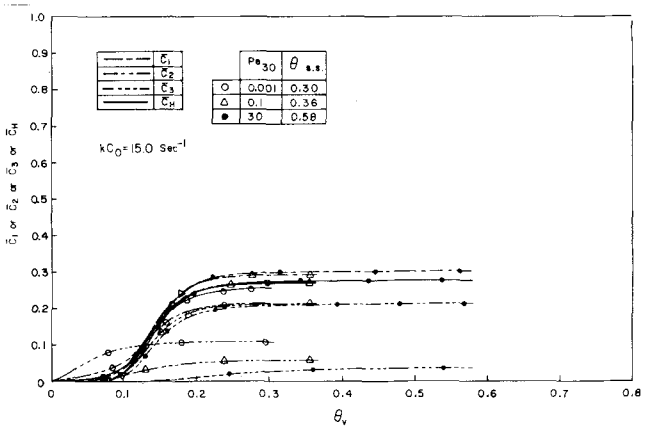

Figure 1(*a*). Effect of Pe_{30} on the concentration variation at the exit of the reactor for $kC_0 = 15.0$ sec^{-1}.

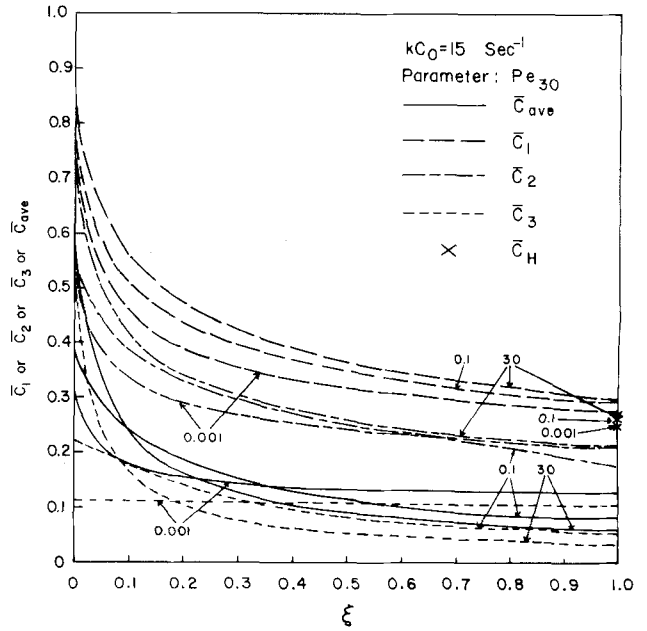

Figure 1(*b*). Effects of Pe_{30} on the concentration distribution at the steady state for $kC_0 = 15$ sec^{-1}.

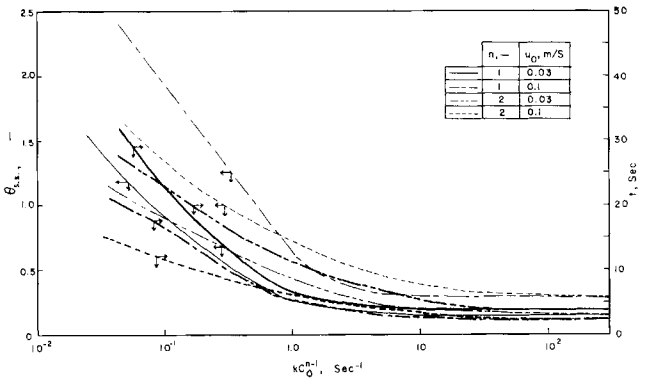

Figure 2. Relationships between $\theta_{s.s.}$ and kC_0^{n-1} as functions of n and U_0.

and

$$\frac{\overline{C}_{avg}\Big|_{\xi=1.0,\,\theta=\theta} - \overline{C}_{avg}\Big|_{\xi=1.0,\,\theta=\theta-\Delta\theta}}{\overline{C}_{avg}\Big|_{\xi=1.0,\,\theta=\theta}} \leq 0.002 \quad (18)$$

Here $\Delta\theta$ is the step size of time integration. $\theta_{s.s.}$ are found to be 0.3, 0.36, and 0.58 for Pe_{30} of 0.991, 0.1 and 30.0, respectively.

The concentration profiles shown in Figure 1*b* indicate that the differences in the gas reactant concentrations among the phases are larger at the inlet than the outlet. A significant amount of the gas reactant in the emulsion phase is converted in the vicinity of the distributor. As expected, the effects of Pe_{30} on the gas concentration distribution in the bubble and cloud phases are not profound. This is due to the fact that a significant amount of the gas reactant is consumed in these two phases prior to its transfer to the emulsion phase, when the rate of chemical reaction is fast.

Duration of Transient Period

To assess the effect of the rate of reaction on the length of the transient period, $\theta_{s.s.}$ is plotted against kC_0^{n-1} as functions of the superficial gas velocity and the order of reaction in Figure 2. The values of the order of reaction considered are 1 and 2. The superficial gas velocities are set at 0.03 and 0.1 m/s. It can be seen that when n is 1 and kC_0 increases from 0.1 to 100 s^{-1}, $\theta_{s.s.}$ decreases monotonically from 1.95 to 0.28 and from 0.9 to 0.16 for U_0 of 0.1 and 0.03 m/s, respectively. When n is 2 and kC_0 increases from 0.1 to 100 s^{-1}, $\theta_{s.s.}$ decreases monotonically from 1.34 to 0.28 and from 0.9 to 0.16 for U_0 of 0.1 and 0.03 m/s, respectively. The rate of decrease in $\theta_{s.s.}$ with respect to the increase in the rate of reaction for a first-order reaction is far more pronounced than that for the second-order reaction at each U_0. When kC_0^{n-1} is large, there is little effect of n on $\theta_{s.s.}$ for a given U_0. This is because for a fast reaction, $\theta_{s.s.}$ is determined predominantly by the residence time of gas in the reactor. $\theta_{s.s.}$ appears to be large for a large U_0 for a given n. However, in the dimensional time time domain (t), it is seen that the situation is reversed. When n is 1 and kC_0 increases from 0.1 to 100 s^{-1}, the values of t decrease monotonically from 23.0 to 3.8 s and from 16.6 to 2.4 s for U_0 of 0.03 and 0.1 m/s, respectively. However, when n is 2 and kC_0 increases from 0.1 to 100 s^{-1}, the values of t decrease monotonically from 23.0 to 3.8 s and from 11.5 to 2.4 s for U_0 of 0.03 and 0.1 m/s, respectively. Note that $\theta_{s.s.}$ of 1 corresponds to 25.5 s for U_0 of 0.03 m/s and 8.5 s for U_0 of 0.1 m/s in the present study.

Model Verification by Means of Experimental Data

Since experimental data are not available for the transient concentration distribution, steady state data are utilized to partially verify the present model. Ozone decomposition data by Kobayashi et al. (1969) as shown in Figures 3*a* through 3*d* are employed here for this purpose. Various values of the physical and operating parameters of their system are reported or estimated as given in Table 3.

To compare the results of the present three-phase model with those of the two-phase model of Kobayashi et al. (1969), the cloud phase in the present model must be lumped into the bubble phase by averaging the concentrations of these two phases as

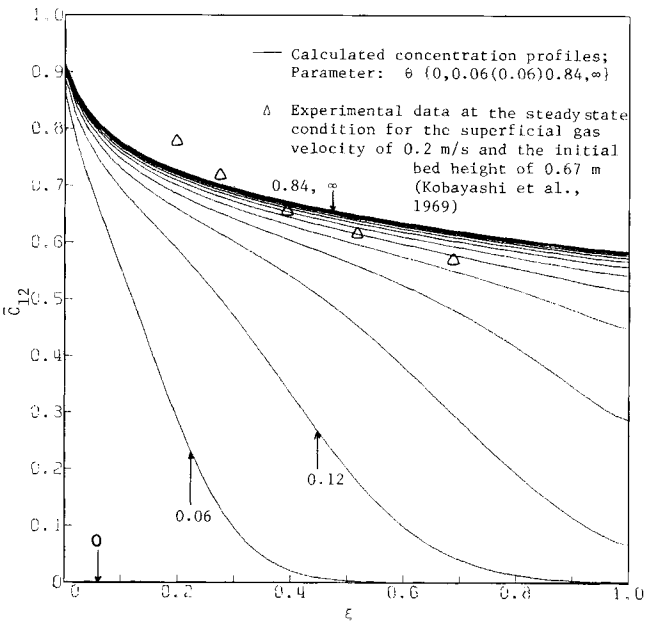

Figure 3(*a*). Comparison of the calculated values and experimental data (Kobayashi et al., 1969) at the steady state, and prediction of the transient profiles for the gas concentration distribution in the bubble-cloud phase for the superficial gas velocity of 0.2 m/s and the initial bed height of 0.67 m.

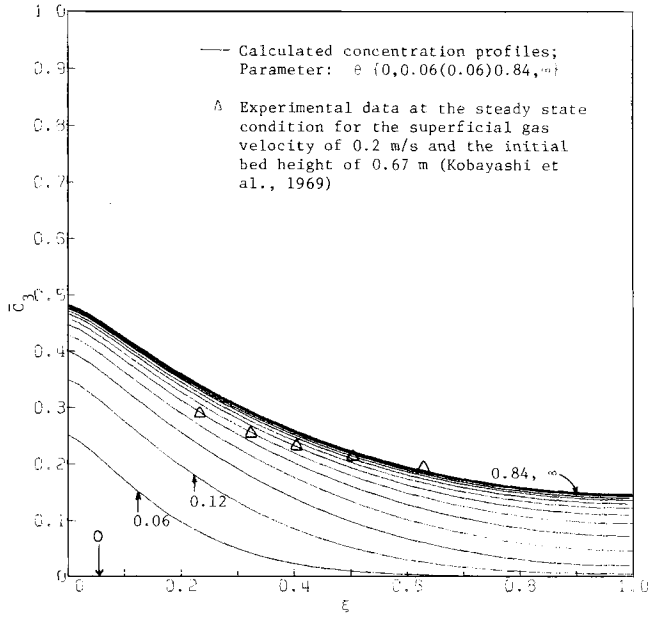

Figure 3(*b*). Comparison of the calculated values and experimental data (Kobayashi et al., 1969) at the steady state, and prediction of the transient profiles for the gas concentration distribution in the emulsion phase for the superficial gas velocity of 0.2 m/s and the initial bed height of 0.67 m.

$$\overline{C}_{12} = \frac{\overline{C}_1\delta_1\epsilon_{1g} + \overline{C}_2\delta_2\epsilon_{2g}}{\delta_1\epsilon_{1g} + \delta_2\epsilon_{2g}} \qquad (19)$$

Figures 3*a*, 3*b*, and 3*c* show the predicted and experimental values of the concentration distributions in the bubble cloud and emulsion phases and the cross-sectional average concentration at the steady state for the superficial gas velocity of 0.2 m/s and the initial bed height of 0.67 m. The predicted transient concentration profiles are also shown in these figures. In Figure 3*d*, the predicted and experimental values of the cross-sectional average concentration distributions and the overall conversion at the steady state are shown for the initial bed height of 0.34 m. The predicted transient concentration profiles are also shown in the figure. Note that the superficial gas velocity is maintained at 0.2 m/s, which is the same as those in Figures 3*a* through 3*c*.

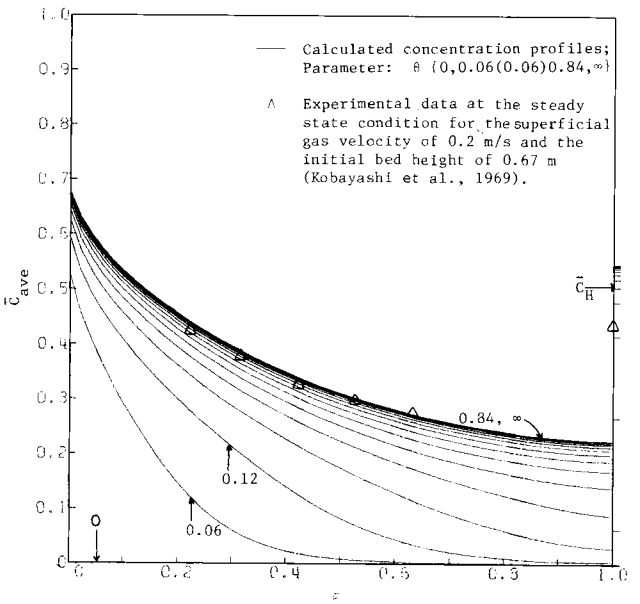

Figure 3(c). Comparison of the calculated values and experimental data (Kobayashi et al., 1969) at the steady state, and prediction of the transient profiles for the average gas concentration distribution in the bed for the superficial gas velocity of 0.2 m/s and the initial bed height of 0.67 m.

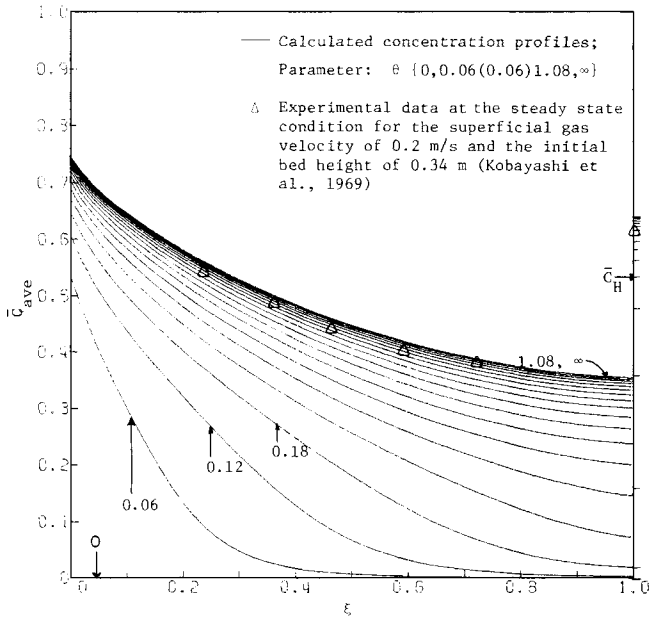

Figure 3*(d)*. Comparison of the calculated values and experimental data (Kobayashi et al., 1969) at the steady state, and prediction of the transient profiles for the average gas concentration distribution in the bed for the superficial gas velocity of 0.2 m/s and the initial bed height of 0.34 m.

The agreement between the predicted and experimental values of the concentration appears to be satisfactory. Pe_{30} in all these figures, that is, Figures 3*a* through 3*d*, remains a constant value of 0.2. Note that Pe_{30} remains a constant for a given fluidized bed in this model.

Although sufficient experimental data in the transient regime are not available to validate the present mechanistic model, we believe that because of the versatility of the present model which takes into consideration the transient characteristics and variable physical properties, it can be effectively utilized to simulate many types of catalytic reactions in fluidized-bed reactors.

CONCLUDING REMARKS

A transient axial dispersion model for isothermal, catalytic, fluidized-bed reactors is presented. This model takes into consideration the significant variations of physical properties along the axial coordinate and the axial dispersion in the three phases, namely, bubble, cloud wake, and emulsion phases, in a fluidized-bed reactor. At the limit of large time, the model approximates the steady state performance of the reactor. Transient and steady state characteristics of the gaseous reactant and the effects of gas mixing have been examined based on the model for the nonlinear chemical reaction. The length of the transient period is evaluated for different reaction rate constants, reaction orders, and superficial gas velocities. The results of numerical simulation of the catalytic fluidized-bed reactor compare favorably with the available experimental data at the steady state condition.

ACKNOWLEDGMENT

This work was supported by the Engineering Experimental Station (Energy Study Project), Kansas State University. The authors wish to acknowledge the assistance of Kei Miyanami on computer programming.

NOTATION

A_t = cross-sectional area, m²
$\overline{C}_{avg}$ = cross-sectional average gas concentration, defined by Equation (15*a*), —
$\overline{C}_i$ = C_i/C_0
$\overline{C}_H$ = volumetric average gas concentration, defined by Equation (15*b*), —
C_i = gas concentration in phase *i*, kg-mole/m³
$\overline{C}_{12}$ = average concentration of gas in the bubble and cloud phases, defined by Equation (19), —
C_{il} = initial gas concentration in phase *i*, kg-mole/m³
C_0 = inlet gas concentration, kg-mole/m³
D_1 = bubble diameter, m
D_G = diffusion coefficient of gas, m²/s
D_t = diameter of the bed, m
D_{1M} = maximum bubble diameter, m
D_{10} = initial bubble diameter at the distributor, m
E_i = axial dispersion coefficient in phase *i*, m²/s
E_{i0} = axial dispersion coefficient in phase *i* evaluated just above the distributor, m²/s
F_{12} = gas exchange coefficient between phase 1 and phase 2 per unit volume of phase 1, 1/s
$\overline{F}_{12}$ = $F_{12}H/U_{10}$
F_{23} = gas exchange coefficient between phase 2 and phase 3 per unit volume of phase 1, 1/s
$\overline{F}_{23}$ = $F_{23}H/U_{20}$

g = gravitational acceleration, m/s^2
H = height of bed expansion, m
$\overline{H}$ = H/H_I
H_I = initial bed height, m
k = reaction rate constant based on the volume of catalysts, 1/s for the first-order reaction and m^3/s/kg-mole for the second-order reaction
n = order ot chemical reaction, —
N_d = number of orifice openings on the distributor, —
Pe_i = Peclet number in phase i, $U_{i0}H/E_{i0}$
Pe_{i0} = $U_{i0}H_I/E_{i0}$
t = time, s
U_i = linear gas velocity in phase i, m/s
$\overline{U}_i$ = U_i/U_{i0}
U_{i0} = linear gas velocity in phase i evaluated just above the distributor, m/s
U_{is} = superficial gas velocity in phase i, m/s
U_{mf} = minimum fluidization velocity, m
U_0 = superficial gas velocity, m/s
x = axial distance from the distributor, m
$\overline{X}$ = overall conversion of the gaseous reactant, —

Greek Letters

δ_i = volume fraction of the bed occupied by phase i, —
ϵ_{mf} = void fraction in the bed at U_{mf}, —
ϵ_{ig} = volume fraction of gas in phase i, based on δ_i, —
ϵ_{is} = volume fraction of solid in phase i, based on δ_i, —
ϵ_I = void fraction at the initial condition, —
ϕ = $\dfrac{kHC_0^{n-1}}{U_0}$
ξ = x/H
ϕ = tU_0/H

Subscripts

i = 1 for the bubble phase, 2 for the cloud wake phase, 3 for the emulsion phase
g = gas
s = solid

LITERATURE CITED

Danckwerts, P. V., "Continuous Flow Systems-Distribution of Residence Time," *Chem. Eng. Sci.*, **2**, 1 (1953).

Davidson, J. F., and D. Harrison, *Fluidized Particles*, Cambridge Univ. Press, England (1963).

Fan, L. T., and L.-S. Fan, "Simulation of Catalytic Fluidized Bed Reactors by a Transient Axial Dispersion Model with Invariant Physical Properties and Nonlinear Chemical Reactions," *Chem. Eng. Sci.*, **34**, 171 (1978).

Fryer, C., and O. E. Potter, "Countercurrent Backmixing Model for Fluidized Bed Catalytic Reactors. Applicability of Simplified Solutions," *Ind. Eng. Chem. Fundamentals*, **11**, 338 (1972*a*).

———, "Bubble Size Variation in Two-Phase of Fluidized Bed Reactors," *Powder Technol.*, **6**, 317 (1972*b*).

Gear, C. W., *Numerical Initial Value Problems in Ordinary Differential Equations*, Prentice-Hall, Englewood Cliffs, N.J. (1971).

Gwyn, J. E., J. H. Moser, and W. A. Parker, "A Three-Phase Model for Gas-Solids Fluidized Beds," *Chem. Eng. Prog. Symposium Ser. No. 101*, **66**, 19 (1970).

Horio, M., and C. Y. Wen, "An Assessment of Fluidized Bed Modeling," *AIChE Symposium Ser. No. 161*, **73**, 9 (1977).

Kato, K., and C. Y. Wen, "Bubble Assemblage Model for Fluidized Bed Catalytic Reactors," *Chem. Eng. Sci.*, **24**, 1351 (1969).

Kobayashi, H., F. Arai, T. Chiba, and M. Matsui, "Concentration Profile in a Gas-Solid Contacting Fluidized Bed," *Kagaku Kogaku Japan*, **33**, 675 (1969).

Kunii, D., and O. Levenspiel, "Bubbling Bed Model. Model for Flow of Gas through a Fluidized Bed," *Ind. Eng. Chem. Fundamentals*, **7**, 446 (1968).

Mori, S., and C. Y. Wen, "Estimation of Bubble Diameter in Gaseous Fluidized Beds," *AIChE J.*, **21**, 109 (1975).

Muchi, I., T. Mamuro, and K. Sasaki, "Studies on the Mixing of Fluid in a Fluidized Bed," *Kagaku Kogaku Japan*, **25**, 747 (1961).

Murray, J. F., "On the Mathematics of Fluidization, Part I Fundamental Equations and Wave Propagation," *J. Fluid Mech.*, **21**, 465 (1965).

Sincovec, R. F., and N. K. Madsen, "Software for Nonlinear Partial Differential Equations," *ACM Trans. Math. Software*, **1**, 232 (1975).

Toomey, R. D., and H. F. Johnstone, "Gaseous Fluidization of Solid Particles," *Chem. Eng. Progr.*, **48**, 220 (1952).

Yoshida, K., T. Mii, and D. Kunii, "Temperature-Effects on the Characteristics of Fluidized Beds," Proceedings of the International Symposium on Fluidization and Its Application, Toulouse (1973).

Zuiderweg, F. J., *Proceedings of the International Symposium on Fluidization*, p. 739, Netherlands University Press, Amsterdam, (1967).

Manuscript received December 11, 1978; revision received February 12, and accepted February 19, 1979.

The Effect of an Expanded Section on Slugging

W.-C. YANG and D. L. KEAIRNS

Research and Development Center
Westinghouse Electric Corporation
Pittsburgh, Pennsylvania 15235

Slugging experiments were performed in a semicircular Plexiglas column 5.6 m in height to study the effect of an expanded section on slugging. The bottom section of the column (3.05 m long) is 28.6 cm in inside diameter and the expanded section 40.6 cm. Both the bed height and the fluidizing velocity were varied during the study, and the results were successfully correlated with a theoretically derived equation. The implications in designing a bed with an expanded section to reduce the slugging effectively are also discussed.

The slugging phenomenon in fluidized beds has been extensively studied and is described in detail by Davidson and Harrison (1971). A slugging bed is characterized by gas slugs of sizes close to reactor cross section that rise at regular intervals and divide the main part of the fluidized bed into alternate regions of dense and lean